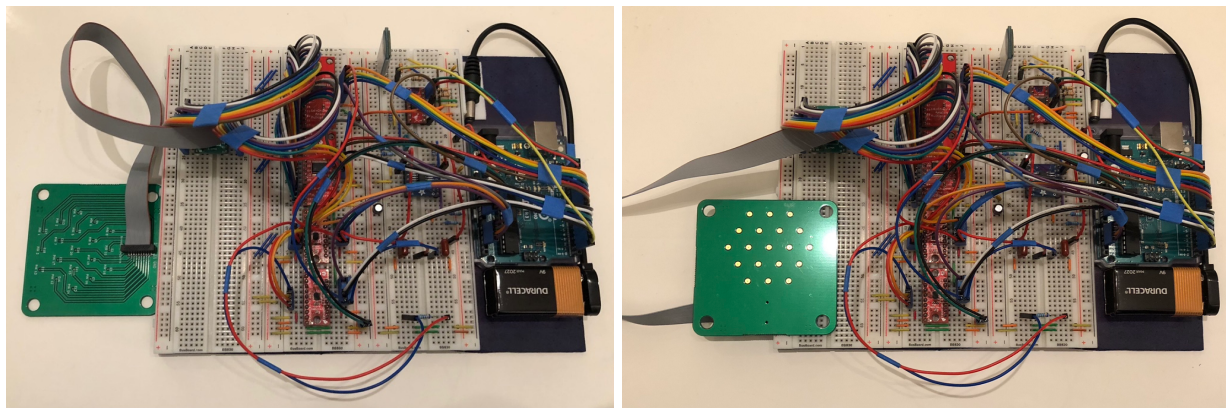


ECE 4781/6781
Final Project Writeup

2D Mapping of Bioimpedance Signals Using Electrode Array for Early Detection of Pressure Ulcers



Professor: Dr. Omer T. Inan
TA: Dongsuk Kang

Keith Liang
Aaron Lim
Sophie Abreu
Yunho Cho
Luke Vanhoozer

Fall 2022

1. Executive Summary

Pressure ulcers are responsible for billions of dollars in healthcare costs and tens of thousands of deaths annually. Because they can develop in as little as a few hours and early damage cannot be seen by the naked eye, early detection of these injuries is essential. In order to address this issue, we have designed a novel bioimpedance measurement and mapping circuit for the early detection of these injuries. The circuit consists of a 19-electrode array, a bioimpedance measurement circuit, analog multiplexers and an Arduino UNO. Bioimpedance measurements are then sent to a PC via bluetooth in order to reconstruct 2D heatmaps of magnitude and phase. Although similar bioimpedance circuits exist in literature, our circuit novelty derives from its portability and elimination of reliance on external measurement equipment for performing measurements (e.g., LCR meter). The largest challenge was designing a bioimpedance measurement circuit small enough for a handheld device while retaining enough accuracy to perform reliable impedance measurements. Additional challenges included designing the electrode array PCB, as well as calibration and integration of the bioimpedance measurement circuit with the multiplexers. Once each subsystem was integrated into the overall system, a program was written in Python to parse bioimpedance data from the Arduino UNO to a PC. Using radial basis function interpolation, the magnitude and phase measurements were plotted to allow for a clear visual representation of the affected area. Several tests were conducted in order to verify the accuracy of our bioimpedance measurement circuit, primarily with a 2R1C circuit and a human forearm using Ag/AgCl electrodes. The results of these two tests verified the accuracy of our circuit and ensured that the skin-electrode interface did not introduce any nonidealities to the system. Once the accuracy of our measurement circuit was verified, we began to take impedance measurements on normal and damaged (burned) porcine skin to see the variation in impedance measurements. We also tested human skin to see the difference in bioimpedance values of normal versus heavily lotioned skin, and both tests yielded successful results with a clear distinction in impedance values between different skin conditions. Several challenges were encountered over the course of testing such as issues with sufficient, even contact of the electrode array on the surface of the skin as well as the ability to accurately mimic pressure ulcer conditions. Future iterations of this project could utilize a flexible silver-tape electrode array as well as a force sensing circuit to quantify the relationship between prolonged pressure and lowered cell impedance. However, with this device's improved usability and simplicity, we believe this could be a future step in developing commercial pressure ulcer detectors in clinical and home settings.

2. Introduction and Significance

Pressure ulcers are skin or soft tissue injuries caused by prolonged pressure exerted over specific areas of the body. This results in reduced blood flow, which can lead to cell death and extreme pain, and an increased risk of the patient developing an infection. Many pressure ulcer injuries heal with treatment, but some never heal completely. They remain a serious health issue within the US, causing more than 60,000 deaths annually. It is estimated that almost 3 million Americans every year develop pressure ulcers, with an estimated additional \$43,000 added to the patient's hospital bill per ulcer. Pressure ulcer related injuries account for 17,000 lawsuits, second only to wrongful death lawsuits, and around \$10 billion in annual US healthcare costs [1]. Pressure ulcers are largely preventable in nature, but due to staffing issues and heavy workloads for nurses, patients may go many hours without being tended to. With early enough detection and proper treatment, billions of dollars and thousands of lives can be saved. In order to improve the quality of pressure ulcer prevention and care, we have designed a portable system for early detection of pressure ulcers using 2D mapping of bioimpedance signals using a multiplexed array of electrodes. This device will allow nurses to more quickly and easily monitor their patient's skin health and give them better foresight to prevent the development of a pressure ulcer.

There are two general categories of pressure ulcer sensors currently in literature. The first type detects prolonged durations of pressure by directly and continuously monitoring pressure. The second type uses bioimpedance measurement to detect the difference in electrical characteristics (e.g., impedance) arising from damaged tissue cells. This is achieved in [2], which utilizes a non-invasive flexible device that maps pressure-induced tissue damage using a multiplexed array of electrodes. We find the second type to be advantageous, since it does not require continuous monitoring, but rather, nurses or caretakers can take periodic measurements to track any accumulation of pressure-induced tissue damage. These bioimpedance devices implement a method called electrical impedance tomography (EIT) which takes advantage of an electrical distinction that exists between healthy and damaged cells to track tissue damage. When normally impermeable cell membranes suffer structural damage from pressure, ions are more easily able to enter and exit the cell. This results in a higher conductance through the cell membrane and a reduced ability to store charge. In other words, damaged cells will exhibit lower overall impedance and behave closer to a resistor than healthy cells. EIT devices track damage by taking multiple impedance measurements over an area of skin. These measurements can be reconstructed in a 2D heat map that identifies damaged areas. Previously reported EIT sensors offer high accuracy and resolution solutions for the mapping [4-6] and even classification [3] of pressure ulcers. However, certain limitations such as physical size and complexity make it difficult for these systems to be produced commercially or used for clinical diagnosis.

3. Project Narrative

3.1. Conception and Ideation

As it is important to detect early signs of pressure damage before visible ulcers begin to form, a robust measurement circuit is required for gathering precise impedance data to distinguish between healthy and damaged skin and tissue cells. In existing works [4-6], this is accomplished by using a benchtop LCR meter and multiplexing through connections between it and unique electrode combinations. However, LCR meters are rather bulky and specialized pieces of equipment that make these systems impractical outside of an experimental setting. Furthermore, the physical wire connections used to connect the circuitry with the LCR meters and provide communication between PCs further limit the mobility and convenience of these designs. The proposed design distinguishes itself from previous works by implementing an on-board circuit for impedance measurements and wireless transmission of this impedance data, therefore eliminating these common drawbacks.

3.2. High Level Architecture

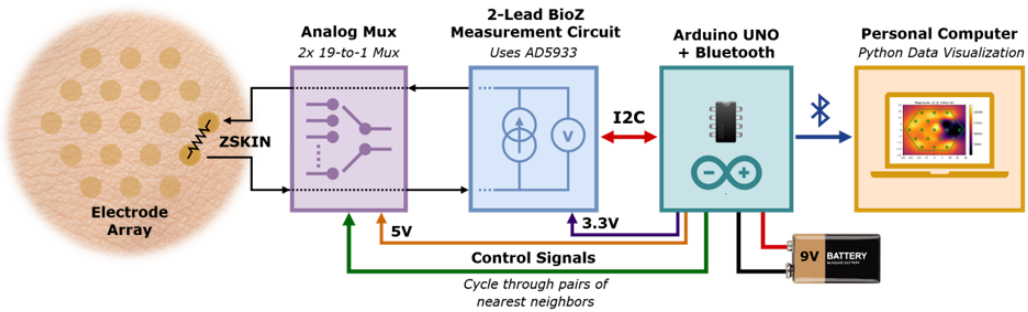


Figure 1. System block diagram of the design that was implemented.

The design can be divided into the 5 subsystems shown in Fig. 1. Skin bioimpedances between pairs of nearest-neighbor electrodes within the **electrode array** are measured one at a time with the **bioimpedance measurement circuit**. **Analog multiplexers** will continuously receive control signals from the **Arduino UNO** to select a pair of electrodes for impedance measurement until all adjacent combinations have been measured. This data is transmitted to a **PC** over Bluetooth, where it will be reconstructed into a heatmap.

While similar in its operation to the designs seen in [4-6], all circuitry in this design can be contained on a single board, while a ribbon cable connects it to the sensor (electrode array). Additional connections to benchtop test equipment and power outlets are not required. This results in a portable, mobile, device that could also feasibly be adapted into a commercial product, further details of which will later be covered in Section 4.

3.3. Electrode Array Design

As the interface between the skin and the measurement circuitry, the electrode array must be carefully designed. With a higher number of electrodes, the array will offer greater resolution for a given area of skin. However, this will further increase the complexity of the analog multiplexing circuit. Therefore, a hexagonal array composed of 19 equidistant electrodes (Fig. 2) was chosen to minimize the circuit's complexity and physical size while still being able to provide a detailed visualization of skin features captured within the electrode array. The electrode array was fabricated on a PCB, where freely-exposed contacts were plated with electroless nickel immersion gold (**ENIG**) to improve electrical conductivity. After testing four different PCB designs with varying pad sizes, it was determined that the PCB with the smallest pad size offered greater consistency between repeated measurement results. Other design considerations included sufficient inter-electrode spacing to prevent gel contact between electrodes, ground-connected copper fills for shielding from electromagnetic interference (EMI), detachable connectors for ease of use, and a thick (1.6 mm) substrate to minimize parasitic capacitance.

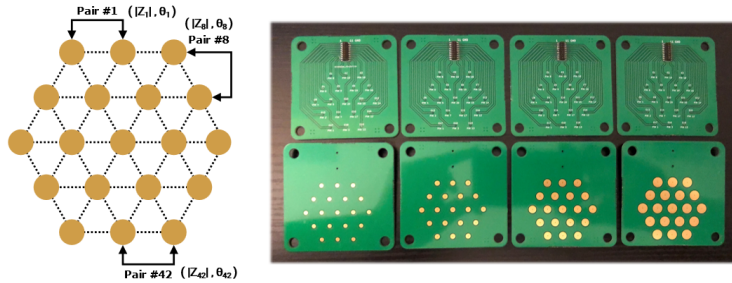


Figure 2. Diagram of electrode array and batch of fabricated PCBs.

Pad diameters (left to right): 2.50mm, 3.25mm, 5.00mm, 6.25mm. Inter-electrode spacing: 10 mm.

3.4. Bioimpedance Measurement

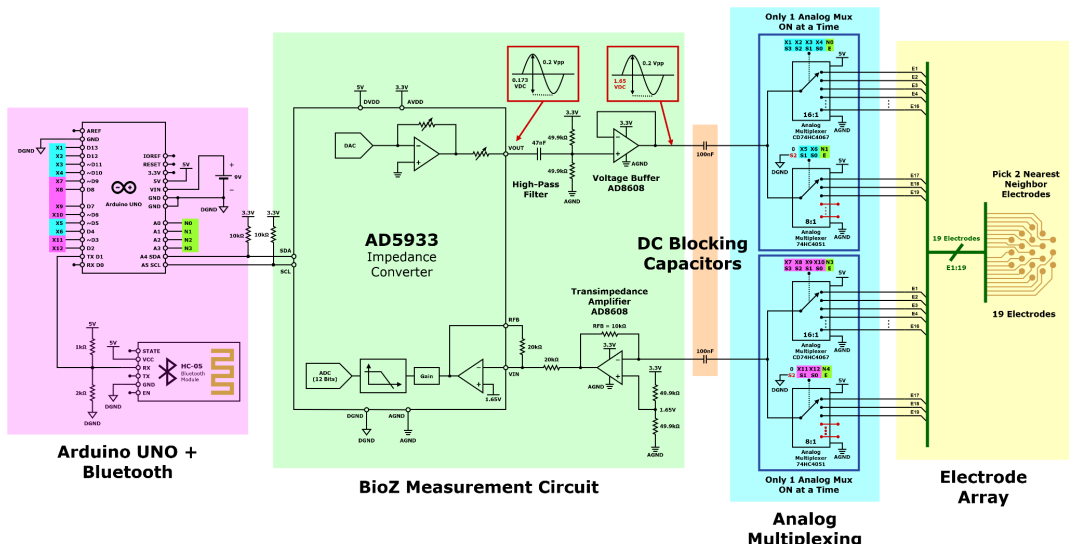


Figure 3. Circuit schematic of design that was implemented.

The bioimpedance measurement circuit and its calibration was the largest design-side challenge of this project. The circuit schematic for this subsystem, shown in Fig. 3, was centered around an AD5933 high precision impedance converter assembled on a single breadboard. In exchange for this improved portability, this solution inevitably sacrifices the high measurement accuracy of a benchtop LCR meter. Therefore, it is important to optimize the analog front end (AFE) circuit for low noise and power, high precision, and most importantly, patient safety.

Since the AD5933 outputs an excitation sine signal with programmable peak-peak voltage and frequency, a high-pass filter was used to filter out non-useful frequencies below 1 kHz. This was used in conjunction with voltage dividers to set the DC voltages of the **Voltage Buffer** at mid-rail to maximize its output range for a sine wave. After being buffered to the AFE's positive load terminal, the filtered sine wave is then passed through the skin using two selected multiplexer channels. 100 nF capacitors were placed between the AFE and the load to block any harmful DC current from being passed through a patient's body, while AC magnitude of the current passing through the skin is converted to a voltage by the **Transimpedance Amplifier** and buffered into the input of the AD5933.

However, the characteristics of the input voltage signal measured by the AD5933 are not only dependent on the skin impedance load, but also by the entire AFE circuit, which will systematically affect the frequency response of the entire signal. Thus, in order to obtain absolute phase and magnitude measurements for the skin itself, these differences introduced by the AFE must be corrected for in software. This was done with an Arduino program that would perform calibration for the AFE circuit connected to a known value resistance and use this data to perform compensation calculations when measuring any new, unknown loads.

For this AFE design, low-noise, low-supply-voltage AD8608 op amps were chosen to limit the effects of noise when measuring weaker signals for high-impedance loads, as well as to operate at the 3.3 V supply from the Arduino. A moderate feedback resistor of 10 k Ω was chosen for the transimpedance amplifier. This value was determined through experimentation, and ensured that the voltage signal inputted to the AD5933 would not clip for the lowest expected load impedance values and maximized the range of higher load impedance values that could be measured. Finally, low-tolerance (0.1%) resistors were used to improve calibration accuracy.

3.5. Analog Multiplexer

The multiplexer circuit is simple in concept; each electrode on the electrode array is connected to both load terminals of the AFE through channels on two analog multiplexers (mux). Select commands from the Arduino are then used to choose two adjacent electrodes, one for each load terminal of the AFE through the skin impedance between the electrodes. This forms a signal path for the bioimpedance measurement circuit. As the objective of this design was to measure the impedance of the skin itself rather than that of the tissue underneath, a two-lead electrode configuration was chosen over one with four leads. Furthermore, a two-lead configuration would offer reduced circuit complexity and area for a more compact system.

However, when choosing the mux components themselves, several important qualities were desired. A low on-resistance is necessary to reduce the impact of additional series resistances on the skin impedance measurements. Additionally, they must be able to operate at a supply voltage of 5V from the Arduino. Finally, the muxes should allow for at least 19 channels to cover each electrode within the array. While components satisfying the first two requirements were readily available, it was difficult to find an analog mux supporting more than 16 channels. As a result, one 16 and one 8 channel mux were used in conjunction as a single mux at both leads of the AFE load to cover 19 electrodes.

While saving on hardware area and cost compared to using a 32 channel mux, this also introduced nonidealities within our measurements. Rather than pass through the same input and output mux for each measurement, the signal will instead pass through one of two input muxes and one of

two output muxes, all with different on-resistances. This is especially problematic when considering that the calibration process for the AFE circuit also uses two of these muxes, leading to improper calibration for electrode measurements that pass through different muxes than the calibration resistor. After performing additional measurements with each electrode pair and known load resistances, as well as considering the small magnitude of the mux on-resistances compared to typical skin impedance values, it was decided that the combined-mux design would not have a significant impact on measurement accuracy. However, the use of a single mux for each electrode would be more ideal in a future design.

3.6. Data Acquisition (PC)

The Arduino uses an HC-05 Bluetooth module to transmit a sequence of impedance and phase measurements to the PC, where it is parsed by a Python script. The script then populates this data into a dense 2D matrix (structured identically to the electrode array) where impedance values of intermediate points are approximated using radial basis function (RBF) interpolation. Ultimately, the values are converted into two heatmap images representing the magnitude and phase of the region.

3.7. Testing and Measurements

3.7.1. 2R1C Circuit Test

In order to verify the accuracy of the AD5933 bioimpedance measurement circuit, we tested it with a 2R1C circuit to mimic skin impedance characteristics. From Fig. 4, we can observe that the measured magnitude and phase responses track the ideal responses fairly well, albeit deviating slightly at higher frequencies. This can be attributed to the impedance of the 2R1C circuit at higher frequencies approaching the minimum measurable impedance limit of our AD5933, which should not pose too much of a challenge for actual skin impedances that typically have much higher impedances.

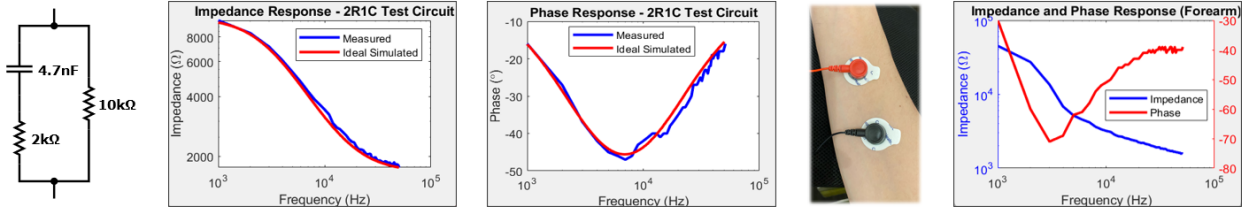


Figure 4. Frequency response of 2R1C circuit and human forearm.

3.7.2. 2-Lead Electrode Test

Following the success of the 2R1C circuit test, we continued to verify the accuracy of our AD5933 bioimpedance measurement circuit by testing it on human skin. In particular, we performed a 2-lead bioimpedance measurement on a human forearm using gold-standard Ag/AgCl wet electrodes. From Fig. 4, we can observe that the overall shape of the magnitude and phase responses bear a close resemblance to the frequency response of the 2R1C model. Therefore, we can conclude that the skin-electrode interface does not introduce any non-idealities over the frequency range we were measuring. Additionally, the measured impedances fell within the established measurements of skin bioimpedances [11], further validating the accuracy of our bioimpedance measurement circuit.

3.7.3. Porcine Skin Test

Once the analog multiplexing circuit was successfully implemented, it was then wired to the AD5933 bioimpedance measurement circuit for system-level testing. There were several different ways of approaching the system-level tests. One such approach was using porcine skin, which previous research [10] has found to be a good substitute for human skin due to their similar thickness. Moreover, since it is also difficult (and unethical) to recreate pressure ulcers on human skin, we used porcine skin to design a variety of repeatable experiments which involve creating burn marks on

porcine skin. Such porcine skin is seen in Fig. 5, where we burnt a small patch of skin on a pig's ear. We initially performed the same procedure on a pig's foot, but due to a lack of surface area for repeated testing, we opted for pig's ears for the rest of our porcine tests.

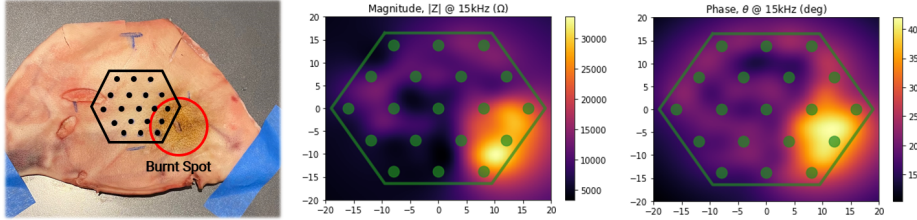


Figure 5. Burnt porcine skin with corresponding magnitude and phase heatmaps.

From Fig. 5, the reconstructed magnitude and phase heatmaps matched relatively well with the burn spot on the pig's ear, which resulted in larger impedance values. This is because burnt skin cells lose their water content and structure due to the immense heat, prohibiting the flow of current by essentially removing the medium in which it propagates through the cells. This ultimately results in a decrease in electrical conductivity, which is reflected in the reconstructed heatmaps.

Additionally, other than blowtorching the porcine skin, we also applied a light application of lotion on it, which we thought would be a more reproducible and systematic testing method. Essentially, lotion should act as a barrier to trap moisture within the skin, which in turn increases a skin's impedance. On the other hand, it may also impede the electrode-skin contact, which should also result in higher impedance measurements. Both of these phenomena were seen in Fig. 6, where the region which lotion was applied to exhibited a higher impedance. Once again, the magnitude and phase heatmaps were comparable to the lotion pattern that was applied on the porcine skin.

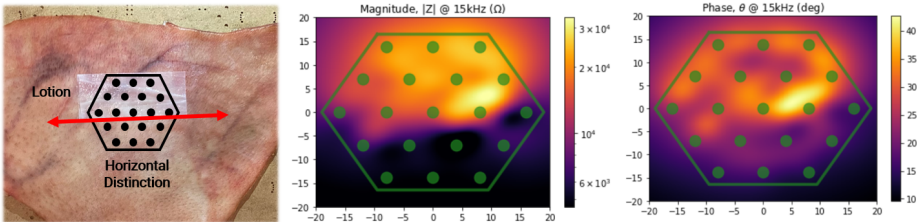


Figure 6. Moisturized porcine skin with corresponding magnitude and phase heatmaps.

3.7.4. Human Skin Test

Aside from testing on porcine skin, we also wanted to test our system on actual human skin. As burning human skin is not a viable option for testing, only lotion was applied to specific areas within the region which the electrode array would interface with the skin. From Fig. 7, the magnitude and phase heatmaps correlate with their respective patterns on the human skin, yielding similar results seen with the porcine skin. Again, the impedance measurements recorded from our system fell within the expected measurements for skin bioimpedance, further validating our overall system.

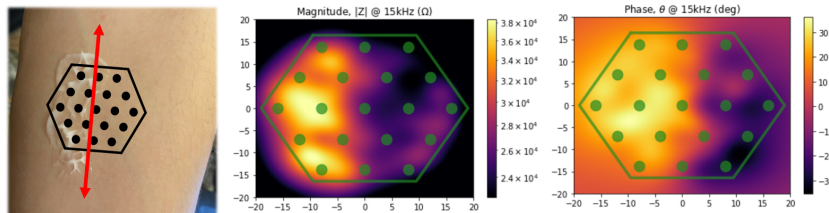


Figure 7. Moisturized human skin with corresponding magnitude and phase heatmaps.

3.7.5. Testing Procedure and Challenges

Several precautionary steps were taken to ensure that reliable magnitude and phase measurements were obtained from our system. For one, electrode gel was applied evenly (shown in Fig. 8) onto the electrode array using an SMT stencil purchased alongside our PCBs. This step was necessary as it ensured that there was good electron-skin contact between the electrode array and the skin under the test, effectively reducing the measured impedance values by a factor of 10. Additionally, for tests involving human skin, Coban wrap (see Fig. 8) was used to ensure that an even amount of pressure was applied on the electrode array to ensure consistent impedance measurements between tests.

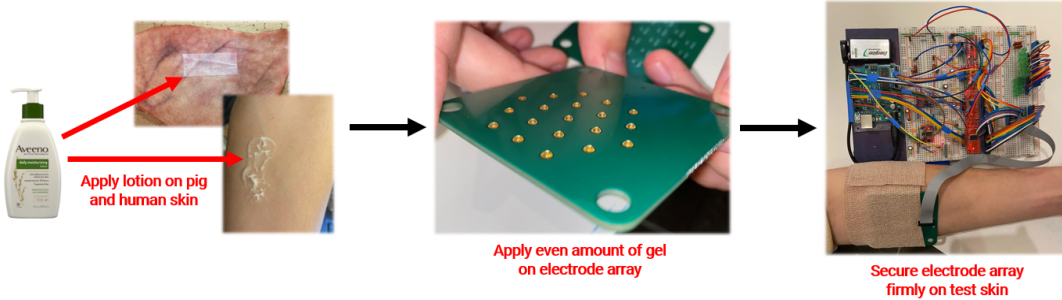


Figure 8. Typical test procedure for human and porcine skin.

The most significant challenge that we encountered during the testing phase was ensuring that the electrode array had good contact with the skin under test. Due to the inherent inflexible nature of the PCB, the electrode array struggled to remain flush on human skin during testing, especially around its edges. Additionally, raised regions of the pig's ear due to cartilage beneath the skin meant that we had to carefully deskin them before any meaningful test.

4. Conclusions and Future Directions

One major challenge during the testing of our system was devising a setup to mimic pressure ulcer damage in a systematic and repeatable way without seriously harming a human subject. Given more time, it would have been possible to implement a force sensing circuit for applying and measuring a quantifiable pressure to human skin over time for our testing. As even skin with mild, reversible pressure damage will exhibit changes in impedance, taking measurements after applying a set (and safe) level of pressure to a human would be a more realistic test environment.

Another challenge faced during testing was the difficulty in taking consistent, accurate measurements. This was due to the fact that the rigid, flat electrode array required steady, even pressure over the entire array, as well as a flat skin surface for measurement. A possible direction that could be explored in a future design is the use of silver-tape fabrication method, where conductive traces are inkjet-printed on a substrate [7]. Silver-tape can be printed on flexible substrates, which would be a useful alternative to rigid, traditional PCBs for aforementioned reasons. Additionally, silver-tape's potential for rapid, low-cost production synergizes well with our concept of a portable, commercial product that can be reused across disposable and detachable electrode arrays between different patients or uses.

5. References

- [1] "Preventing Pressure Ulcers in Hospitals." *Agency for Hospital Research and Quality*. Retrieved from ahrq.gov/patient-safety/settings/hospital/resource/pressureulcer/tool/pu1.html
- [2] Swisher, S. L., Lin, M. C., Liao, A., Leeflang, E. J., Khan, Y., Pavinatto, F. J., Mann, K., Naujokas, A., Young, D., Roy, S., & others. (2015). Impedance sensing device enables early detection of pressure ulcers in vivo. *Nature Communications*, 6(1), 1–10.
- [3] S. Kang, S. Noyori, H. Noguchi, T. Takahashi, H. Sanada and T. Mori, "Development of an Electrical Impedance Tomography Spectroscopy for Pressure Ulcer Monitoring Tool: Preliminary study," 2020 42nd Annual International Conference of the IEEE Engineering in Medicine & Biology Society (EMBC), 2020, pp. 5073-5076, doi: 10.1109/EMBC44109.2020.9176256.
- [4] Ching, C. T.-S., & Chen, J.-H. (2015). A non-invasive, bioimpedance-based 2-dimensional imaging system for detection and localization of pathological epithelial tissues. *Sensors and Actuators B: Chemical*, 206, 319–326. [https://doi.org/https://doi.org/10.1016/j.snb.2014.09.072](https://doi.org/10.1016/j.snb.2014.09.072)
- [5] A. Liao et al., "Impedance sensing device for monitoring ulcer healing in human patients," 2015 37th Annual International Conference of the IEEE Engineering in Medicine and Biology Society (EMBC), 2015, pp. 5130-5133, doi: 10.1109/EMBC.2015.7319546.
- [6] S. Liu, Y. Xu, S. Chen, Q. Hu and F. Dong, "Detection of Pressure Ulcers Using Electrical Impedance Tomography," 2022 IEEE International Instrumentation and Measurement Technology Conference (I2MTC), 2022, pp. 1-6, doi: 10.1109/I2MTC48687.2022.9806603.
- [7] Cheng, T., Narumi, K., Do, Y., Zhang, Y., Ta, T. D., Sasatani, T., Markvicka, E., Kawahara, Y., Yao, L., Abowd, G. D., & others. (2020). Silver tape: Inkjet-printed circuits peeled-and-transferred on versatile substrates. *Proceedings of the ACM on Interactive, Mobile, Wearable and Ubiquitous Technologies*, 4(1), 1–17.
- [8] Fernandes, I. J., Aroche, A. F., Schuck, A., Lamberty, P., Peter, C. R., Hasenkamp, W., & Rocha, T. L. (2020). Silver nanoparticle conductive inks: Synthesis, characterization, and fabrication of inkjet-printed flexible electrodes. *Scientific Reports*, 10(1), 1–11.
- [9] "1 msps, 12-bit impedance converter, Network Analyzer Data sheet AD5933," *AD5933 (Rev. F)*. [Online]. Available: <https://www.analog.com/media/en/technical-documentation/data-sheets/AD5933.pdf>. [Accessed: 01-Nov-2022].
- [10] A. Summerfield, F. Meurens, and M. E. Ricklin, "The immunology of the porcine skin and its value as a model for human skin," *Molecular Immunology*, vol. 66, no. 1, pp. 14–21, 2015.
- [11] D. J. Bora and R. Dasgupta, "Estimation of skin impedance models with experimental data and a proposed model for human skin impedance," *IET Systems Biology*, vol. 14, no. 5, pp. 230–240, 2020.